Carbon dioxide dynamics from sediment, sediment-water interface and overlying water in the aquaculture shrimp ponds in subtropical estuaries, southeast China

Carbon dioxide dynamics from sediment, sediment-water interface and overlying water in the aquaculture shrimp ponds in subtropical estuaries, Southeast China

Ping Yang,[1,2,3] Derrick Y F. Lai,[4] Hong Yang,[5,6,7] Chuan Tong[1,2,3]

[1]Key Laboratory of Humid Subtropical Eco-geographical Process of Ministry of Education, Fujian Normal University, Fuzhou 350007, P.R. China

[2]School of Geographical Sciences, Fujian Normal University, Fuzhou 350007, P.R. China

[3]Research Centre of Wetlands in Subtropical Region, Fujian Normal University, Fuzhou 350007, P.R. China

[4]Department of Geography and Resource Management, The Chinese University of Hong Kong, Shatin, New Territories, Hong Kong SAR, China

[5]Collaborative Innovation Center of Atmospheric Environment and Equipment Technology，Jiangsu Key Laboratory of Atmospheric Environment Monitoring and Pollution Control, School of Environmental Science and Engineering, Nanjing University of Information Science & Technology, 219 Ningliu Road, Nanjing 210044, China

[6]College of Environmental Science and Engineering, Fujian Normal University, Fuzhou, 350007, China

[7]Department of Geography and Environmental Science, University of Reading, Whiteknights, Reading, RG6 6AB, UK

***Correspondence to:** Ping Yang
Telephone: 086-0591-87445659
Fax: 086-0591-83465397
Email: yangping528@sina.cn (P. Yang)
****Correspondence to:** Chuan Tong
Telephone: 086-0591-87445659
Fax: 086-0591-83465397
Email: tongch@fjnu.edu.cn (C. Tong)

A B S T R A C T

Aquaculture ponds can emit a large amount carbon dioxide (CO_2), with the consequence of exacerbating global climate change. Many studies about CO_2 dynamics across the water-air interface, but CO_2 in sediment and overlying water received relative less attention. In this study, CO_2 concentration in sediment porewater, the diffusive CO_2 fluxes across the sediment-water interface (SWI), and the CO_2 production rates in the overlying water (CO_{2_WP}) were determined in the shrimp ponds in the Min River Estuary (MRE) and Jiulong River Estuary (JRE), southeast China, to analyze the dynamics of CO_2 among different growth stages of shrimps. Our results showed large variations in porewater CO_2 concentrations, CO_2 diffusive fluxes and CO_{2_WP} rates among different growth stages, with markedly larger values in the middle stage of shrimp growth. The temporal variation of CO_2 in both estuarine ponds followed closely the seasonal change of temperature. The internal CO_2 production (CO_{2_IP}) in these ponds was dominated by sediments. A significantly larger mean porewater CO_2 concentrations, diffusive fluxes and production rate were observed in the MRE ponds than in the JRE ponds, which could be attributed to the lower water salinity and a larger source of carbon substrates in the former estuary. Considering a total surface area of 6.63×10^3 km^2 across the mariculture ponds in subtropical estuaries, it is estimated conservatively that approximately 100 Gigagram (Gg) of dissolved organic carbon and 190 Gg of dissolved inorganic carbon were transported annually from the mariculture ponds into China's coastal areas. Because of the substantial supply of dissolved carbon, the adjacent coastal waters receiving effluent discharge from the mariculture ponds could become "hotspots" of CO_2 emissions. Our results highlight the role of aquaculture pond as a major CO_2 source in China's coastal areas, and effective actions are needed to alleviate the greenhouse gases (GHGs) emissions in these areas.

Keywords: Carbon dioxide; Sediment-water interface; Production rates; Mariculture ponds; Subtropical estuary

Nomenclature table

Nomenclature	Abbreviations	Nomenclature	Abbreviations
Greenhouse gases	GHGs	CO_2 production rates in the overlying water	CO_{2_WP}
Gigagram	Gg	Internal CO_2 production	CO_{2_IP}
Dissolved organic carbon	DOC	CO_2 production at the sediment by microbial mineralization	CO_{2_SP}
Dissolved inorganic carbon	DIC	CO_2 production in the water column by photochemical mineralization	CO_{2_PP}
Total carbon	TC	CO_2 production in the water column by and heterotrophic respiration of shrimps	CO_{2_SR}
Chlorophyll *a*	Chl-*a*	Two-way analysis of variance	ANOVA
Sediment-water interface	SWI	Repeated measures analysis of variance	RMANOVA
Min River Estuary	MRE	Principal component analysis	PCA
Jiulong River Estuary	JRE		

1. Introduction

The increasing worldwide concerns over global climate change and its effects on ecosystem and human society call for a better understanding of the magnitude of greenhouse gas (GHGs) emissions (Tong et al., 2010; Yang et al., 2011). Carbon dioxide (CO_2) is one of the most potent GHGs, accouting for nearly 60% of the overall radiative forcing in the air (Mosier, 1998; Myhre et al., 2013). Global atmospheric CO_2 concentration has increased from 280 ppm in 1750 to 405 ppm in 2017, exceeding the pre-industrial levels by about 40% (World Meteorological Organization, 2018). Aquatic ecosystems (e.g. lakes, reservoirs, rivers, and others) are known to be important sources of atmospheric CO_2. Earlier estimates indicate that inland freshwaters could emit in the order of 1.4 Pg C $year^{-1}$ in the form of CO_2 (Tranvik et al., 2009), equivalent to approximately 55% of terrestrial carbon sink (Raymond et al., 2013; Tangen et al., 2016). Yet, accurate estimates of regional and global CO_2 budgets remains challenging because of large uncertainty regarding aquatic CO_2 emissions due to insufficient measurements. Shallow waters, including aquaculture ponds, have recently been highlighted as key hotspots for CO_2 emissions (Holgerson and Raymond, 2016; Yang et al., 2018b). Quantifying the potential sources of various aquatic ecosystems has become one of the top priorities for improving the prediction of future CO_2 emission.

In response to the urgent need of climate change mitigation, there has been an increasing number of studies in recent years to explains on the impacts of aquaculture systems on carbon cycle (e.g. Chen et al., 2015; Chen et al., 2016; Sidik and Lovelock, 2013; Yang et al., 2018b). However, the majority of these studies only focused on CO_2 fluxes across the water-air interface of aquaculture ponds, with little attention on the CO_2 fluxes across the sediment-water interface (SWI) (Xiong et al., 2017). CO_2 production can takes place either in anaerobic sediments or in aerobic water columns (Gruca-Rokosz et al., 2011; Xing et al., 2005); unfortunately, there is a lack of research on CO_2 production rates in the aerobic water column of aquaculture ponds. It is important to note that CO_2 fluxes across the water-air interface are not necessarily equivalent to the CO_2 fluxes across the SWI, due to the fact the actual proportion of CO_2 emitted to the atmosphere is also influenced by microbiological processes in water column (Gruca-Rokosz and Tomaszek, 2015; Xing et al., 2006; Yang et al., 2008). Therefore, studying the CO_2 dynamics across the SWI and quantifying the CO_2 production rates in the overlying water is crucial to improve our understanding of the overall carbon balance of aquaculture ponds and its resulting impacts on global warming.

According to the recent statistics, approximately 90% of the global aquaculture production occurs in Asia (FAO, 2014). In particular, China has world's largest mariculture industry (Gu et al., 2017a, 2017b), with a total mariculture pond area and production of 2.57×10^4 km^2 and 2.30×10^9 kg in 2015, which representing approximately 30% of the world total of pond area and 60% of the world total of aquaculture production (Chen et al., 2016). Land-based aquaculture is the one of dominant approaches of mariculture shrimp production (FAO, 2014). Mariculture ponds are generally semi-artificial ecosystems, with a large amount of organic matter

supply from daily input of feeds (Chen et al., 2015; Yang et al., 2018a). The decomposition of organic matter from residual feeds and feces in these ponds can stimulate CO_2 production and emissions (Burford et al., 2003; Chen et al., 2016). Aquaculture ponds are inherently heterogeneous over spatiotemporal scales due to the changes in topographic features, environmental conditions, and tidal fluctuations, leading to large uncertainties in the calculation of CO_2 production and emissions. Unfortunately, the spatiotemporal variability of CO_2 production and emissions from mariculture ponds are nearly unknown, which could cause biases in the estimation of the contribution of mariculture activities to radiative forcing and global. In the current research, we aim to fill these knowledge gaps by analyzing the CO_2 dynamics in aquaculture ponds between two subtropical estuaries in Fujian Province, which is one of the main distribution centers of shrimp produce in China.

2. Materials and methods

2.1. Study area description

This study was conducted in the Min River Estuary (MRE) and Jiulong River Estuary (JRE) located in southeastern China (Fig. 1; Yang et al., 2018). The MRE has a typically subtropical monsoon climate, warm and wet in summer, with annual precipitation of 1,350 mm and annual mean temperature of 19.6°C (Tong et al., 2010). The JRE is in the subtropical oceanic climate zone. The mean annual rainfall is 1,371 mm and annual air temperature is 21.0°C (Wang et al., 2013). Both estuaries receive a greater amount of precipitation during the period between May and September owing to the southeast monsoon. Tides in both estuaries are semi-diurnal. The surface wetland soil is submerged for approximately 7 h during a 24 h cycle. The mean salinities of tidal water in MRE and JRE are approximately 4.2±2.5 ppt (Tong et al., 2012) and 21.3±2.9 ppt, respectively. Shrimp pond, one of the main landscapes in the estuarine zones, was mostly created by removing marsh vegetation.

2.2. Shrimp pond system and management

Because the optimal water temperatures to culture shrimp (*Litopenaeus vannamei*) are 22–35ºC, only one crop of shrimp could be produced annually at MRE and JRE (Yang et al., 2017a). The shrimp production cycle began in the second half of May and lasted for six months. Before the shrimp production, the ponds were filled with salt water pumped from an adjacent estuary. To prevent shrimp's predators and competitors, the water was also passed through a 2-mm mesh bag (Guerrero-Galván et al., 1999; Yang et al., 2017a). Freshwater was added into the ponds in rainy days. After shrimp harvesting, water was discharged from the pond spillways. During the culture period, water levels in shrimp ponds ranged 1.1–1.5 m and 1.3–1.8 m in MRE and JRE, respectively.

Shrimps were fed with artificial feeds containing 42% crude protein (Yuehai™, China) in the morning (07:00) and afternoon (16:00) by direct application on the boat. According to water quality, pond management practices, and shrimp weight, the shrimp growth cycle was divided into three stages: initial, middle, and final stages (Yang et al., 2017a). Three to five 1,500-W paddlewheel aerators were operated four times daily (07:00–09:00, 12:00–14:00, 18:00–20:00, and 00:00–03:00) in the ponds. Detailed information on the shrimp pond systems and management

practices was reported in a previous study (Yang et al., 2017a). To analyze CO_2 dynamics in the culture period, water and sediment were sampled from three representative shrimp ponds at Shanyutan Wetland in MRE and the Humao Island in JRE, respectively (Fig. 1). Basic details of the selected mariculture ponds in the two estuaries are presented in Table S1.

2.3. Collection and analysis of water and sediment samples

2.3.1. Collection and analysis of water samples

Field sampling campaigns were performed in June, August, and October 2015 which represented three culture stages (initial, middle, and final). Sampling was performed on different but consecutive days (less than six days between the two estuaries) in any sampling campaign. Overlying water samples were collecteded from three sites in each pond. Overlying water was sampled at approximately 5 cm above the bottom sediments using a 5-L Niskin water sampler. Water samples were stored in an ice box, and transported to the laboratory within 4 h for incubation and measurement of water quality parameters within one week (Yang et al., 2017a). A portion of the water samples was filtered through a 0.45 μm cellulose acetate filter (Biotrans™ nylon membranes). The filtrates were subsequently analyzed for dissolved organic carbon (DOC) and dissolved inorganic carbon (DIC) using a Shimadzu total organic carbon analyzer (TOC-V, Yang et al., 2017a). Chl-*a* concentrations in water samples were determined using a UV-visible spectrophotometer (Shimadzu UV-2450, Japan) following the methods of Jeffrey and Humphrey (1975) and Yang et al. (2017a). In addition, during each sampling campaign, the overlying water temperature and pH were determined using a pH/mV/Temp system (IQ150, IQ Scientific Instruments, USA), the salinity was measured using a salinity meter (Eutech Instruments-Salt6, USA) and DO was measured using a multi-parameter water quality meter (HORIBA, Japan).

2.3.2. Collection and analysis of sediment samples

Four intact sediment cores were sampled at each of the triplicate sites in each pond using a surface-operated coring device (Core-60, Austria). The device is composed of a core cylinder, a plexiglas tube (30 cm length, 6 cm internal diameter) and a one-way check valve which can preserve the integrity of 15 cm sediment and 15 cm overlying water (Yang et al., 2017a). The cores were sealed, stored vertically in an ice box, and transported to the laboratory within 4 h. In the laboratory, the four replicate sediment cores collected at each site were used separately for incubation experiments, and the measurement of sediment physicochemical properties, dissolved CO_2 concentrations, and physicochemical variables of sediment porewater. Sediment temperature were measured using a handheld pH/mV/temperature meter (IQ150, IQ Scienti fic Instruments, USA). Sediment porosity (Φ) was calculated based on the water content of sediment determined by weight loss after drying at 105°C for 24 h (Zhang et al., 2013). Applying a soil-to-water ratio of 1:2.5 (w/v), sediment pH was determined using a pH meter (Orion 868, USA). After freeze drying, homogenization and grinding to fine power (Sun et al., 2013), sediment was analyzed for total carbon (TC) using an elemental analyzer (Elementar Vario MAX CN, Germany). Porewater was extracted from the bulk sediment by centrifugation at

5,000 rpm for 10 min (Cence® L550, De Vittor et al., 2012). The extracted porewater samples were divided into two portions. One portion of the porewater samples was filtered through 0.45 μm pore size cellulose acetate filters (Biotrans™ nylon membranes) (De Vittor et al., 2012) and the filtrates were analyzed for DOC and DIC concentrations, while the other unfiltered portion was measured for salinity using an Eutech Instruments-Salt6 salinity meter.

To measure the dissolved CO_2 concentrations in sediment porewater, 6 cm^3 of sediment subsamples were collected in duplicate with 10 mL cut-off syringes and sealed in serum vials containing 24 mL of CO_2-free water and 0.5 mL of saturated $HgCl_2$ solution. The mixtures were shaken to achieve gas equilibrium between the slurry and the headspace (Dutta et al., 2015). Finally, the headspace CO_2 concentration was analyzed using a gas chromatograph (GC-2010, Shimadzu, Kyoto, Japan). The CO_2 concentration in porewater (C, mg CO_2 L^{-1}) was calculated using the following equation (Ding et al., 2010; Johnson et al., 1990):

$$C = (C_h / 22.4) \times [(\beta \times R \times T) / 22.4 + (V_h / V_p)] \times (M / 1000) \quad (1)$$

where C_h is the CO_2 concentration in vial headspace (mL L^{-1}); β is the Bunsen solubility coefficient for CO_2 (L L^{-1}) (Wiesenburg and Guinasso, 1979); R is the gas constant (0.0814); T is the room temperature (°C); M is molar mass of CO_2 (mg mol^{-1}); and V_h and V_p are the volumes of vial headspace volume (mL) and water sample (mL), respectively.

2.4. Laboratory incubation for the determination of CO_2 production and flux rates

The CO_2 production rates in the overlying water and CO_2 fluxes across the SWI were determined by *ex situ* incubation. The incubation device (Fig. S1) was constructed following the guide of Chen et al. (2014), Xiong et al. (2017), and Yang et al. (2017a). Intact core samples containing equal volumes of sediments and overlying water were transported to the laboratory within 4 h after collection and placed in incubation chambers for 2 h to re-establish the equilibrium conditions (Xiong et al., 2017). After reaching an equilibrium, the incubation chambers were carefully filled with overlying water using a rubber pipe (Fig. S1) (Yang et al., 2017a), with special attention being paid to maintain a sufficiently low water flow rate to avoid any disturbance of the sediment surface. After filling the incubation chambers with overlying water, the cores were sealed with a Teflon plunger equipped with inlet and outlet tubes (Fig. S1). The overlying water was continuously bubbled with air to simulate the *in situ* oxic conditions of water above the sediment (Mu et al., 2017), and overlying water were stirred during incubation. The chambers were then incubated in a temperature-regulated incubator device (QHZ-98A, China) for 9 h (Yang et al., 2017a). The incubation temperature was set to be the same as the field temperature (MRE: 22.5, 28.5, and 22.5 °C in June, August, and October, respectively; JRE: 25.5, 29.0, and 26.5 °C in June, August, and October, respectively). 60 mL of water samples were withdrawn from each chamber near the SWI using a 100 mL plastic syringe at 0 h, 3 h, 6 h, and 9 h of the incubation period. Subsequently, water samples were transferred to headspace vials to determine dissolved CO_2 concentrations using a gas chromatograph (Shimadzu GC-2010,

Japan) based on the gas-stripping method (Zhang et al., 2010a). After each water sampling, the same volume of field-collected overlying water was introduced into the chamber (Fig. S1) to replace the sampled water and maintain the total volume of the water column in the incubation chamber. In addition, we incubated bottom water without any sediment under the same conditions in a separate chamber to estimate the CO_2 production rate in bottom water.

Dissolved CO_2 concentration in water samples was estimated by applying Henry's law and taking into account the dependence of gas solubility on water temperature and salinity (Lide and Frederikse, 1997; Wanninkhof et al., 1992). The CO_2 flux across the sediment-water interface (SWI) (mg m^{-2} h^{-1}), and CO_2 production rate in bottom water (CO_{2_WP}, mg m^{-2} h^{-1}) were calculated based on the CO_2 concentration changes in the water column over incubation time (Equation 2) (Xiong et al., 2017; Zheng et al., 2009):

$$\mathrm{CO_2flux(or\ CO_{2\_WP})} = \frac{d\mathrm{c}}{d\mathrm{t}} \times V \times S \times (M/1000) \qquad (2)$$

where $\frac{d\mathrm{c}}{d\mathrm{t}}$ is the rate of change in CO_2 concentrations in the overlying water (mmol L^{-1} h^{-1}); V is the volume of overlying water in the incubation chamber (L); S is the cross-sectional area of the sediment core (m^2); and M is molar mass of CO_2 (mg mol^{-1}). Positive values of CO_2 fluxes indicate a net CO_2 release from sediments into the water column, whereas negative values indicate a net CO_2 uptake by sediments from the water column.

2.5. Statistical analysis

Two-way analysis of variance (ANOVA) was conducted to analyze the influences of estuaries and culture stages and the interaction between the two factors on sediment porewater CO_2 concentrations, CO_2 flux across the SWI, and CO_{2_WP}. Repeated measures analysis of variance (RMANOVA) was operated to examine the differences in environmental variables of shrimp ponds between these two estuaries during the study period, with the data collected in a given estuary over the three stages of shrimp growth being the repeated measures. Pearson correlation analysis was conducted to estimate the relationships (1) between porewater CO_2 concentrations, CO_{2_WP}, or CO_2 flux and environmental variables, and (2) between CO_2 fluxes and the gradient of CO_2 concentrations in both sediment porewater and the overlying water. Principal component analysis (PCA) was also performed to analyze relationships among the CO_2 production rates (or CO_2 fluxes) and observed environmental parameters and to show their pattern at different aquaculture stages. A stepwise regression analysis was further used to screen the major influential environmental factors for the temporal variations of CO_2 production rates in overlying water and CO_2 fluxes across the SWI from different estuarine ponds. All statistical analyses were performed using the SPSS statistical software package (SPSS v 22.0, IBM, Armonk, NY, USA) and the statistical results at the level of 0.05 were considered as significance. The results were presented as average ± 1 standard error. Statistical plots and conceptual diagrams were generated using OriginPro 7.5

(OriginLab Corp. USA).

3. Results and Discussion

3.1. Surface sediment, porewater, and overlying water characteristics

The characteristics of surface sediments in the shrimp ponds of the two estuaries over the study period are shown in Fig. 2a–c. The minimum and maximum sediment temperatures were recorded at initial and middle stages, respectively. Significant differences in mean temperature were detected between the two estuaries at all three periods (p<0.05) (Fig. 2a). Sediment porosity at MRE was significantly lower at the initial stage than middle and final stages (p<0.05) (Fig. 2b), while at JRE, significantly higher porosity was observed during the middle stage (p<0.05) (Fig. 2b). The average sediment porosity was significantly higher at JRE than MRE over the study period (p<0.01). A similar seasonal trend was observed for sediment TC content in the shrimp ponds, with considerably smaller and larger results at initial and middle stages, respectively (Fig. 2c). Although the temporal patterns of sediment TC at MRE and JRE were very similar, significant differences in mean values were observed between the two estuaries in all three periods (p<0.01) (Fig. 2c). Meanwhile, the mean TC values found in our ponds were within the range of 1.08-5.43% observed across 233 aquaculture ponds around the world (Boyd et al., 2010). The mean sediment pH values at ponds in MRE and JRE were 6.9±0.1 and 6.3±0.1, respectively. The seasonal changes of sediment pH at ponds in two estuaries followed the order of initial stage < final stage < middle stage.

The characteristics of sediment porewater in the shrimp ponds are shown in Fig. 2d–f. The temporal patterns of porewater salinity were very similar in the two estuaries, with a generally decreasing trend over the study period (Fig. 2d). Due to a greater input of freshwater (e.g., terrestrial/estuarine groundwater, precipitation), JRE had significantly higher porewater salinity than MRE (p<0.01). Porewater DOC concentration reached a minima and a maxima in October and August, respectively, while significant differences in mean DOC concentrations between the two estuaries were detected in both June and August (p<0.01) (Fig. 2e). The lowest and highest porewater DIC concentrations were detected in June and August, respectively, with no significant differences between the two estuaries at all times (p<0.05) (Fig. 2e). The variations in various environment variables in the overlying water during the shrimp growth cycle are shown in Fig. 2. The bottom water had pH values ranging 8.4–10.2 at MRE and 8.2–9.8 at JRE (Fig. 3a), with significant differences between estuaries at initial and final stages (p<0.05), and significantly lower pH at middle stage (p<0.05). DO concentrations in the pond water of both estuaries showed an increasing trend over time (Fig. 3b). The concentrations of DOC and DIC in JRE ponds increased with time, while those in MRE ponds were significantly higher during the middle stage (p<0.05; Fig. 3c and 3d). The mean water DOC and DIC concentrations at MRE ponds were 12.6±0.3 mg L^{-1} and 21.9±1.2 mg L^{-1}, respectively, which were significantly higher than those at JRE ponds (6.7±0.4 mg L^{-1} and 16.2±0.7 mg L^{-1}, respectively, p<0.01).

3.2. Porewater dissolved CO_2 concentrations

The concentrations of dissolved CO_2 in the sediment porewater are shown in

Fig. 4a. The mean porewater CO_2 concentrations at MRE and JRE ponds during the study period were 4.9±0.6 and 2.1±0.6 mg L^{-1}, respectively, with a range of 4.4-6.0 and 0.9-3.1 mg L^{-1}, respectively. The porewater CO_2 concentrations at MRE and JRE demonstrated similar seasonal trends, with higher and lower values at the middle and final stages, respectively (Fig. 4a and Table 1). CO_2 concentration shared the similar patterns with temperature and porewater DOC in sediments (p<0.05 or p<0.01) (Fig. 2a and 2e, and Table 2), indicating that temperature, organic matter, and their interactions were important factors influencing the variability of porewater CO_2 concentrations in shrimp ponds. The CO_2 in porewater was predominantly produced by the degradation of organic matter (Gruca-Rokosz and Tomaszek, 2015; Wollast, 1993). The presence of a large amount of organic matter would supply a large amount of substrates to microbes for the soil C mineralization (Kristensen et al., 2008; Yang et al., 2012), with the possible consequence of increase in porewater CO_2 levels. Furthermore, a higher temperature could greatly enhance microbial decomposition of soil organic matter (Golovatskaya and Dyukarev, 2009; Lafleur et al., 2005), and thus the release of CO_2 from sediments into the porewater. Our results suggested that the high sediment temperature and the large organic matter associated with the high bait feeding and intense metabolic activity of shrimps (Burford et al., 2003) would contribute to the elevated porewater CO_2 concentrations observed in the middle stage compared to initial and final stages. The strong and negative correlations found between pH and porewater CO_2 concentrations (Table 2) further suggested that the temporal variations in sediment porewater CO_2 concentrations might partly depend on pH changes. Our results were in agreement with those of previous studies conducted in aquatic ecosystems (e.g. Crawford et al., 2013; Neal et al., 1998; Wallin et al., 2010), especially in shallow aquaculture ecosystems (Chen et al., 2016; Xiong et al., 2017).

Porewater CO_2 concentrations varied significantly between MRE and JRE across these three shrimp growth stages (p<0.001) (Table 1), with generally high and very low values for MRE and JRE ponds, respectively (Fig. 4a). One possible reason for this spatial variations could be attributed to the differences in sediment TC contents and porewater DOC concentrations (Fig. 2c and 2e, and Table 1), which was in line with the earlier discussion of the effects of organic matter on sediment CO_2 production. In the present study, MRE ponds had much lower porewater salinity than JRE ponds (Fig. 2d), which could be a result of freshwater dilution caused by the interactions between precipitation and surface runoff. Combining two estuaries together, porewater CO_2 concentration were negatively correlated with porewater salinity (r=0.54, p<0.01), indicating that salinity was another important factor influencing the porewater CO_2 concentrations in the estuarine ponds. High salinity has been suggested to inhibit the activities of, or even bring harm to, microorganisms, which would subsequently reduce carbon mineralization rates and CO_2 production (Hu et al., 2017).

3.3. Production rates of CO_2 in overlying water

The culture of aquatic fauna in mariculture ponds is supported by daily supply of feeds (Chen et al., 2016). These ponds accumulate a large amount of organic

carbon from residual feeds and feces (Burford et al., 2003; Chen et al., 2016), which supported significant CO_2 production arising from the microbial decomposition of organic matter in the aerobic water column and subsequently the release of CO_2 from aquaculture ponds into the atmosphere as shown by our data. Fig. 4b shows our laboratory incubation experiment results about the production rates of CO_2 in the overlying water. There was a clear temporal variation of CO_2 production rates in all the mariculture ponds during the study period (p<0.001, Table 1). The CO_2 production rates in MRE ponds ranged between 14.5 and 22.0 mg m^{-2} h^{-1}, with significantly smaller values during the initia and final stages than middle stage (p<0.01). The CO_2 production rates in JRE ponds ranged 3.9-15.8 mg m^{-2} h^{-1}, with significantly lower results at the initial stage (p<0.01, Fig. 4b). Chen et al. (2015) observed similar temporal patterns in grass carp *Ctenopharyngodon idella* polyculture ponds, and suggested that temperature, Chl-*a* (Chlorophyll *a*) concentrations, and water temperature played a primary role in controlling CO_2 production. Some studies also reported a considerable temporal variability in CO_2 production rates in the freshwater environment and wetland sediments (e.g. Almeida et al., 2016; Vachon et al., 2016; Weyhenmeyer et al., 2015), which was mainly governed by seasonal variability in temperature and organic matter concentrations (Hu et al., 2017; Vachon et al., 2016). However, the results of our principal component analysis showed that the temporal variations in CO_2 production rates were primarily related to different sets of environmental variable between sites (Fig. 5). In MRE ponds, the CO_2 production rate was significantly related to DOC (R = 0.84, p<0.01) and temperature (R = 0.72, p<0.01) (Fig. 5a), which together accounted for 76.1% of the variance in CO_2 production rates (Table 3). In JRE ponds, however, the temporal patterns of overlying water CO_2 production rates were mainly driven by salinity (R = 0.76, p<0.01) and DIC concentration (R^2 = 0.72, p<0.01) (Fig. 5b), which together accounted for 68.7% of the variance in CO_2 production (Table 3). Salinity was a significant factor affecting CO_2 production in JRE but not MRE, which could be related to the much lower baseline salinity level and hence a greater sensitivity of microbial activities to salinity changes in the former estuary. In contrast, CO_2 production in the more saline MRE ponds was more strongly controlled by the supply of organic substrates (e.g. DOC) for microbial mineralization.

The production rates of CO_2 in the overlying water also varied markedly between the two estuaries (Fig. 4b). The mean CO_2 production rate in MRE was significantly higher than that in JRE ponds (17.6±1.3 vs. 10.6±1.3 mg m^{-2} h^{-1}, p<0.001, Table 1). The conversion of natural coastal wetlands to aquaculture ponds conceals or eliminates the spatial heterogeneity, topographic features, and hydrological characteristics of the habitats (Yang et al., 2017b). However, the magnitude of chemical parameters measured in the pond overlying water varied significantly between the two estuaries. In particular, significant differences in salinity, DOC, and DIC concentrations between MRE and JRE ponds were observed (p<0.05 or p<0.01) (Fig. 2d, and Fig. 3c, 3d). The survival rate and the densities of shrimps and baits were the major factors affecting DOC and DIC concentrations in mariculture ponds (Yang et al., 2018a). Considering high density of shrimps, a large

amount of bait was added into the ponds in MRE. However, the low survival rate of shrimps (MRE vs. JRE: 65% vs 71%) had resulted in a substantial accumulation of surplus baits, which would decompose and contribute to high DOC and DIC concentrations in the water column (Fig. 3c and Fig. 3d). In addition, the lower salinity in MRE arising from the greater amount of freshwater runoff could contribute to the enhanced CO_2 production in the ponds (Fig. 4b). In contrast, the JRE ponds had a higher water salinity but a lower bait concentration as a result of a lower density and a higher survival rate of shrimps, which together led to both lower organic matter content and CO_2 production rates as compared to MRE (Fig. 4b). Our results showed that local environmental conditions affecting the physico-chemical properties of shrimp pond water (e.g. organic matter, salinity, and others) were important driver causing the observed difference in CO_2 production rates between ponds.

3.4. Fluxes of CO_2 across the sediment-water interface

CO_2 fluxes across the SWI are shown in Fig. 4c. The relationships between CO_2 fluxes and the environmental variables are also shown in two separate PCA plots, which demonstrated the temporal patterns in MRE (Fig. 5c) and JRE ponds (Fig. 5d), respectively. The CO_2 fluxes from ponds in MRE and JRE were high, ranging between 43.6 and 97.7 mg m^{-2} h^{-1} and between 20.2 and 99.9 mg m^{-2} h^{-1}, respectively. Significant differences in mean CO_2 fluxes were recorded among the three shrimp growth stages (p<0.001, Table 1) and the highest values was detected in the middle stage (Fig. 4c). The temporal variations in pond CO_2 fluxes between the two estuaries were influenced similarly by sediment temperature (MRE: R^2=0.38, p<0.01; JRE: R^2=0.69, p<0.01; also see Fig. 5 and Table 4) and sediment TC level (MRE: R^2=0.17, p<0.05; JRE: R^2=0.31, p<0.01), implying that the importance of temperature for the mineralization of organic matter and CO_2 fluxes across the SWI (Table 4 and Fig. 5). Xiong et al. (2017) also reported that an increase in temperature could stimulate soil microbial activities and carbon mineralization, resulting in an oversaturation of CO_2 and hence a large release of CO_2 from the sediments to the overlying water. Moreover, this study found that the temporal changes in CO_2 fluxes across the SWI were similar to those of the gradient of CO_2 concentrations between the porewater and overlying water over the study period (Fig. 6), indicating that the CO_2 diffusive gradient could at least in part govern the variations in CO_2 flux among the three stages of shrimp growth. Some recent studies further suggested that *L. vannamei* in the aquaculture ponds could affect carbon transport and transformation in surface sediments because the depth of sediment bioturbation caused by this shrimp was up to 2 cm (Xiong et al., 2017; Zhong et al., 2015). The different intensities of bioturbation among the three shrimp growth stages might also contribute to the observed seasonal changes of CO_2 fluxes across the SWI.

Over the study period, the mean CO_2 flux across the SWI in the MRE ponds was 63.68±6.56 mg m^{-2} h^{-1}, greater than that in the JRE ponds (54.36±7.70 mg m^{-2} h^{-1}). The variation patterns of CO_2 flux and porewater CO_2 concentration were highly similar (Fig. 4a and 4c; r^2=0.40, p<0.001), which is consistent with that of previous findinds that high GHG emissions are associated with high porewater GHG

concentrations (Tong et al., 2018; Xiang et al., 2015; Zhang et al., 2010b). The magnitude of CO_2 fluxes from our estuarine ponds was also different from that of other aquatic ecosystems (Table 5). The average values and the range of CO_2 fluxes observed in our shrimp pond systems were substantially larger than those reported in lakes (Casper et al., 2003; Liikanen et al., 2002; Ogrinc et al., 2002; Yang et al., 2015a) and reservoirs (Gruca-Rokosz et al., 2011; Gruca-Rokosz and Tomaszek, 2015). The CO_2 fluxes across the SWI from the shrimp ponds in our two estuaries were also higher than those from the subtropical rivers or estuaries, such as the Mississippi River Estuary, USA (Morse and Rowe, 1999) and the Shanghai river network, China (Tan, 2014), but generally lower than those from the drainage ditches in the Netherlands (Schrier-Uijl et al., 2011) and the intertidal mudflats in Japan (Kikuchi, 1986). Meanwhile, the magnitude of CO_2 fluxes in our study was similar to that in the freshwater aquaculture systems in China (Xiong et al., 2017), which suggested that the sediments of mariculture ponds could be potential "hotspots" of CO_2 emissions, and the role of mariculture ponds should be taken into account when evaluating the CO_2 balance of aquatic ecosystems.

The high CO_2 fluxes across the SWI observed in our shrimp ponds were, to some extent, related to the large supply of organic matter. These mariculture ponds were often maintained through daily feed application to culture the target aquatic fauna (Chen et al., 2015, 2016). In fact, the feed utilization efficiency is unfortunately as low as 4.0–27.4% (Chen et al., 2015; Molnar et al., 2013), so only a limited proportion of the feed inputs could be converted into fish biomass. Very likely majority of the added feeds would end up accumulating in the mariculture systems (Chen et al., 2015; Yang et al., 2017a), leading to the generation of a large amount of organic residues, mainly uneaten feeds, during mariculture production that in turn stimulate microbial decomposition and subsequently CO_2 production and emission from mariculture ponds.

3.5. Implications and future outlook for carbon biogeochemical cycling

3.5.1. Role of sediments in the internal CO_2 production of shrimp ponds

Decomposition or mineralization of organic matter plays a crucial role in the internal CO_2 production in aquatic ecosystems (Müller et al., 2015; Vreča, 2003). According to Weyhenmeyer et al. (2015), the internal CO_2 production (CO_{2_IP}) comprised of three different processes, namely CO_2 production at the sediment by microbial mineralization (CO_{2_SP}), CO_2 production in the water column by microbial mineralization of DOC (CO_{2_WP}), and CO_2 production in the water column by photochemical mineralization (CO_{2_PP}). Numerous studies reported that CO_{2_WP} often made the largest contribution to the internal CO_2 production in the boreal lakes (e.g. Almeida et al., 2016; Brothers et al., 2012; Weyhenmeyer et al., 2015). Weyhenmeyer et al. (2015) reported that the median CO_2 production rate in over 5,000 boreal lakes generally followed the order of CO_{2_WP} (221 mg C m^{-2} d^{-1}) > CO_{2_SP} (47 mg C m^{-2} d^{-1}) > CO_{2_PP} (25.6 mg C m^{-2} d^{-1}), with significantly higher values in autumn. Similarly, Algesten et al. (2005) reported that CO_{2_SP} played a minor role in the production and emissions of CO_2 in the boreal and subarctic lakes in the summer. In the present study, CO_2 release fluxes across the SWI and CO_{2_WP}

in the shrimp ponds ranged between 20.2 and 99.9 mg m^{-2} h^{-1}, and between 3.9 and 22.0 mg m^{-2} h^{-1}, respectively. The mean CO_2 release fluxes across the SWI in the two estuarine ponds was over 3.9 times larger than the CO_{2_WP} rate (58.9 vs. 14.9 mg m^{-2} h^{-1}, $p<0.01$), which suggested that sediment CO_2 production contributed substantially to the total production and emissions of CO_2 in subtropical aquaculture ponds during the culture period. The relative larger contribution of CO_{2_SP} to the CO_{2_IP} in subtropical shrimp ponds is different from that in the boreal and subarctic lakes. There were two possible mechanisms that could account for the considerable impacts of sediments on the CO_2 balance in the current study. First, the pond sediment received a large quantity of organic carbon from residual feeds and feces (Chen et al., 2016; Yang et al., 2017a) that served as important substrates to microbes for decomposition and subsequent CO_2 production. Second, the shallow water depth (an average of 1.5 m) and the operation of paddlewheel aerators would effectively promote the diffusion of oxygen from the water into the sediment (Silva et al., 2013; Yang et al., 2017a), which in turn enhance aerobic respiration and the microbial decomposition of sediment organic matter.

3.5.2. Impact of pond effluent on CO_2 dynamics in receiving coastal waters

In the end of aquaculture production, pond water is complete drained to discard the aquaculture wastewater and aerate the bottom sediments to prepare for the next production (Herbeck, et al., 2013; Yang et al., 2017a). During this management practice, large quantities of nutrient-enriched water would be transferred into the adjacent coastal zone over a short period (Wu et al., 2014), with a serious consequence of water pollution, eutrophication and other damages to the environment (Yang, 2014). Annual discharge of total nitrogen (TN) and total phosphorus (TP) from shrimp mariculture into the Min River Estuary was estimated to 30.45 and 2.40 Mg, respectively (Yang et al., 2017a). Consequently, TN and TP concentrations in the receiving waters jumped markedly by 270% and 234%, respectively (Yang et al., 2017a). This study further estimated that the annual discharge of DOC and DIC from shrimp mariculture into the adjacent coastal waters was 444.1 and 706.2 Mg, respectively, for MRE (the total pond area of 26.30 km^2, water depth of 1.4 m, and mean DOC and DIC concentrations of 13.5 and 21.5 mg L^{-1}, respectively) and 550.2 and 1264.1 Mg, respectively, for JRE (a total pond area of 43.3 km^2, water depth of 1.5 m, and mean DOC and DIC concentrations of 8.3 and 18.9 mg L^{-1}, respectively). Considering the total area of China's subtropical estuaries mariculture of 6.6×10^3 km^2 (Yao et al., 2016) and a mean water depth of 1.4 m and assuming that our data were representative of the mariculture ponds across China, it is estimated that approximately 100 Gg DOC y^{-1} and 190 Gg DIC y^{-1} would be directly discharged from the mariculture ponds into the adjacent coastal zone. The decomposition of organic matter such as DOC was the main driver of the internal CO_2 production in aquatic ecosystems (Müller et al., 2015; Weyhenmeyer et al., 2016). The discharge of aquaculture effluents can rapidly alter the supply of organic matter and the quality of nearby waters (Herbeck et al., 2013; Yang et al., 2017c), which subsequently create a favorable environment for CO_2 production internally in the coastal ecosystems. Our results pointed to the potential of adjacent

receiving coastal waters in the effluent discharge area of the ponds being potential "hotspots" of CO_2 emissions in winter.

3.5.3. Management to reduce CO_2 emission from aquaculture ponds

Yang et al. (2018) found variations in CO_2 emissions fluxes across the water-air interface from aquaculture ponds among estuaries, with high fluxes in Min River Estuary (17.47 mg m^{-2} h^{-1}) and low fluxes in Jiulong River Estuary (15.40 mg m^{-2} h^{-1}). The variation of CO_2 emission fluxes was similar to those of porewater CO_2 concentrations (Fig. 4a), overlying water CO_2 production rates (Fig. 4b) and sediment CO_2 release rates (Fig. 4c). The result indicate that high CO_2 emissions were accompanied by high CO_2 production and porewater CO_2 concentrations. The high variation of CO_2 emission and other biogeochemical processes from mariculture ponds is commonly related to multiple environmental factors, but low salinity is necessary to produce high CO_2 production and emission fluxes. This implies that increasing salinity level of aquaculture ponds might be an measure to reduce CO_2 emission from aquaculture, but the potential impact to other environmental conditions should be monitored and minimized. From 1 January 2015, China has started the new Environmental Protection Law (EPL) and the strict implementation of EPL and related regulations will be the key for the sustainable development of aquaculture in China (Yang, 2014; Yang et al., 2015b).

3.5.4. Limitation and future research

Similar as many studies, there are some limitations in the current study. It should be noted that large uncertainties might exist in our estimated contributions of CO_{2_SP} and CO_{2_WP} to the overall CO_{2_IP} rate of aquaculture ponds owing to the limited size of our data sets with only two estuaries. Future research should increase the frequency of *in situ* sampling, for example the diurnal change (Xing et al., 2004), and include more innovative techniques, to measure CO_{2_SP} and CO_{2_WP} in aquaculture ponds at multiple spatial scales. Future long-term *in situ* sampling and monitoring with multiple frequencies in various regions of China should be carried out to obtain a more complete picture of the influence of aquaculture pond effluents on CO_2 production and emissions in coastal ecosystems. Furthermore, the aquaculture pond ecosystem is characterized by shallow water depth, high transparency, and high daily feed supply, which together could provide a suitable environment for CO_2 production in the water column by photochemical mineralization (CO_{2_PP}) and heterotrophic respiration of shrimps (CO_{2_SR}). While CO_{2_PP} and CO_{2_SR} are likely important contributors to the internal CO_2 production in subtropical aquaculture ponds, the roles of CO_{2_PP} and CO_{2_SR} deserve further investigation. In the current study, CO_2 fluxes were analyzed completely based on laboratory incubation experiments, and further *in situ* experiments will be helpful to unravel the detailed mechanisms of bioturbation on CO_2 efflux.

4. Conclusions

Carbon dioxide production from sediment and overlying water at aquaculture shrimp ponds in two subtropical estuaries were research in the current study. Significant differences in porewater CO_2 concentrations, CO_{2_WP}, and CO_2 fluxes across the SWI were observed at the shrimp ponds in subtropical estuaries among

growth stages, with much higher values in the middle stage. Our results suggested that the seasonal variations in sediment temperature and organic matter supply were the key drivers of the changes in porewater CO_2 concentrations and CO_2 fluxes, while the temporal variations of CO_{2_WP} were governed by the interactions between organic matter and other abiotic factors (e.g. pH and salinity). Higher porewater CO_2 concentrations and CO_{2_WP} in the MRE than the JRE ponds could be partly attributed to the difference in salinity levels between the two estuaries. Our results further highlighted the importance of considering the variability of CO_2 production among different estuaries and aquaculture stages in order to produce reliable extrapolation and estimates of large-scale carbon balances. The mean CO_2 fluxes across the SWI in the ponds was approximately 3.9 times larger than the mean CO_{2_WP} rate, suggesting that sediment was an important contributor to the internal CO_2 production at the shrimp ponds in subtropical estuaries. Therefore, formulating management strategies in minimizing sediment CO_2 release would be crucial for reducing CO_2 emissions from aquaculture ponds to the atmosphere in future.

Acknowledgments

This research was financially supported by the National Science Foundation of China (No. 41801070, 41671088), the Graduate Student Science and Technology Innovation Project of the School of Geographical Science of the Fujian Normal University (GY201601), the Research Grants Council of the Hong Kong Special Administrative Region, China (CUHK458913, 14302014, 14305515), the CUHK Direct Grant (SS15481), Open Research Fund Program of Jiangsu Key Laboratory of Atmospheric Environment Monitoring & Pollution Control, and Minjiang Scholar Programme. We would like to thank Yi-fei Zhang, and Li-shan Tan of the School of Geographical Sciences, Fujian Normal University for their field assistance.We sincerely thank Prof., David Bastviken for valuable suggestions.

References

Adams, D.D. 2005. Diffuse flux of greenhouse gases-methane and carbon dioxide-at the sediment-water interface of some lakes and reservoirs of the world. In: Tremblay A, Varfalvy L, Roehm C, Garneau M [eds.] Greenhouse gas emissions-fluxes and processes. Springer, Berlin, p 129-153.

Algesten, G., Sobek, S., Bergström, A.K., Jonsson, A., Tranvik, L.J., Jansson, M., 2005. Contribution of sediment respiration to summer CO_2 emission from low productive boreal and subarctic lakes. Microb. Ecol. 50, 529-535. doi: 10.1007/s00248-005-5007-x

Almeida, R.M., Nóbrega, G.N., Junger, P.C., Figueiredo, A.V., Andrade, A.S., de Moura, C.G.B., Tonetta, D., Oliveira Jr., E.S., Araújo, F., Rust, F., Piñeiro-Guerra, J.M., Mendonça Jr., J.R., Medeiros, L.R., Pinheiro, L., Miranda, M., Costa, M.R.A., Melo, M.L., Nobre, R.L.G., Benevides, T., Roland, F., de Klein, J., Barros, N.O., Mendonça, R., Becker, V., Huszar, V.L.M., Kosten, S., 2016. High primary production contrasts with intense carbon emission in a eutrophic tropical reservoir. Front. Microbiol. 7, 717. doi: 10.3389/fmicb.2016.00717

Boyd, C.E., Wood, C.W., Chaney, P.L., Queiroz, J.F., 2010. Role of aquaculture pond sediments in sequestration of annual global carbon emissions. Env. Poll. 158, 2537-2540. doi: 10.1016/j.envpol.2010.04.025

Brothers, S.M., Prairie, Y.T., Del Giorgio, P.A., 2012. Benthic and pelagic sources of carbon dioxide in boreal lakes and a young reservoir (Eastmain-1) in eastern Canada. Glob. Biogeochem. Cycles. 26, GB1002. doi: 10.1029/2011GB004074

628 Burford, M.A., Thompson, P.J., McIntosh, R.P., Bauman, R.H., Pearson, D.C., 2003. Nutrient
629 and microbial dynamics in high-intensity, zero-exchange shrimp ponds in Belize.
630 Aquaculture 219, 393-411. doi: 10.1016/S0044-8486(02)00575-6
631 Casper, P., Furtado, A., Adams, D.D., 2003. Biogeochemistry and diffuse fluxes of greenhouse
632 gases (methane and carbon dioxide) and dinitrogen from the sediments in oligotrophic
633 Lake Stechlin. In: Koschel, R., Adams, D.D., (Eds) Lake Stechlin: an approach to
634 understand an oligotrophic lowland lake. Arch. Hydrobiol. Spec. Iss. Adv. Limnol. 58,
635 53-71.
636 Chen, Y., Dong, S.L., Wang, F., Gao, Q.F., Tian, X.L., 2016. Carbon dioxide and methane fluxes
637 from feeding and no-feeding mariculture ponds. Env. Poll. 212, 489-497. doi:
638 10.1016/j.envpol.2016.02.039
639 Chen, Y., Dong, S.L., Wang, Z.N., Wang, F., Gao, Q.F., Tian, X.L., Xiong, Y.H., 2015. Variations
640 in CO_2 fluxes from grass carp *Ctenopharyngodon idella* aquaculture polyculture ponds.
641 Aquacult. Environ. Interact. 8, 31-40. doi: 10.3354/aei00149
642 Crawford, J.T.,Striegl, R.G., Wickland, K.P., Dornblaser, M.M., Stanley, E.H., 2013. Emissions
643 of carbon dioxide and methane from a headwater stream network of interior Alaska. J.
644 Geophys. Res. Biogeosci. 118, 482-494. doi: 10.1002/jgrg.20034
645 De Vittor, C., Faganeli, J., Emili, A., Covelli, S., Predonzani, S., Acquavita, A., 2012. Benthic
646 fluxes of oxygen, carbon and nutrients in the Marano and Grado Lagoon (northern
647 Adriatic Sea, Italy). Estuar. Coast. Shelf S. 113, 57-70. doi: 10.1016/j.ecss.2012.03.031
648 Ding, W.X., Zhang, Y.H., Cai, Z.C., 2010. Impact of permanent inundation on methane emissions
649 from a *Spartina alterniflora* coastal salt marsh. Atmos. Environ. 44, 3894-3900. doi:
650 10.1016/j.atmosenv.2010.07.025
651 Dutta, M.K., Mukherjee, R., Jana, T.K., Mukhopadhyay, S.K., 2015. Biogeochemical dynamics
652 of exogenous methane in an estuary associated to a mangrove biosphere; The
653 Sundarbans, NE coast of India. Mar. Chem. 170, 1-10. doi:
654 10.1016/j.marchem.2014.12.006
655 FAO, 2014. The State of World Fisheries and Aquaculture. Food and Agricultural Organization
656 of the United Nations, Rome, Italy.
657 Golovatskaya, E.A., Dyukarev, E.A., 2009. Carbon budget of oligotrophic mire sites in the
658 Southern Taiga of Western Siberia. Plant. Soil. 315, 19-34. doi:
659 10.1007/s11104-008-9842-7
660 Gruca-Rokosz, R., Tomaszek, J.A., 2015. Methane and carbon dioxide in the sediment of a
661 eutrophic reservoir: production pathways and diffusion fluxes at the sediment-water
662 interface. Water. Air. Soil. Poll. 226, 16. doi: 10.1007/s11270-014-2268-3
663 Gruca-Rokosz, R., Tomaszek, J.A., Koszelnik, P., Czerwieniec, E., 2011. Methane and carbon
664 dioxide fluxes at the sediment-water interface in reservoirs. Polish J. Environ. Stud.
665 20(1), 81-86.
666 Gu, Y.G., Ouyang, J., Ning, J.J., Wang, Z.H., 2017a. Distribution and sources of organic carbon,
667 nitrogen and their isotopes in surface sediments from the largest mariculture zone of the
668 eastern Guangdong coast, South China. Mar. Pollut. Bull. 120, 286-291. doi:
669 10.1016/j.marpolbul.2017.05.013
670 Gu, Y.G., Ouyang, J., An, H., Jiang, S.J., Tang. H.Q., 2017b. Risk assessment and seasonal
671 variation of heavy metals in settling particulate matter (SPM) from a typical southern
672 Chinese mariculture base. Mar. Pollut. Bull. 123, 404-409. doi:
673 10.1016/j.marpolbul.2017.08.044
674 Guerrero-Galván, S.R., Páez-Osuna, F., Ruiz-Fernández, A.C., Espinoza-Angulo, R., 1999.
675 Seasonal variation in the water quality and chlorophyll *a* of semi-intensive shrimp ponds
676 in a subtropical environment. Hydrobiologia. 391, 33-45. doi: 10.1023/A:100359062
677 Hansen, K., Kristensen, E., 1997. Impact of macrofaunal recolonization on benthic metabolism
678 and nutrient fluxes in a shallow marine sediment previously overgrown with macroalgal
679 mats. Estuar. Coast.Shelf S. 45(5), 613-628. doi: 10.1006/ecss.1996.0229
680 Herbeck, L.S., Unger, D., Wu, Y., Jennerjahn, T.C., 2013. Effluent, nutrient and organic matter
681 export from shrimp and fish ponds causing eutrophication in coastal and back-reef
682 waters of NE Hainan, tropical China. Cont. Shelf Res. 57, 92-104. doi:
683 10.1016/j.csr.2012.05.006

Holgerson, M.A., Raymond, P.A., 2016. Large contribution to inland water CO_2 and CH_4 emissions from very small ponds. Nat. Geosci. 9, 222-226. doi: 10.1038/NGEO2654

Hu, M.J., Ren, H.C., Ren, P., Li, J.B., Wilson, B.J., Tong, C., 2017. Response of gaseous carbon emissions to low-level salinity increase in tidal marsh ecosystem of the Min River estuary, southeastern China. J. Environ. Sci. 52, 210-222. doi: 10.1016/j.jes.2016.05.009

Jeffrey, S.W., Humphrey, G.F., 1975. New spectrophotometric equations for determining chlorophylls *a*, *b*, c_1 and c_2 in higher plants, algae and natural phytoplankton. Biochemie und Physiologic der Pflanzen. 167, 191-194. doi: 10.1016/0022-2860(75)85046-0

Johnson, K.M., Hughes, J.E., Donaghay, P.L., Sieburth, J.M., 1990. Bottle-calibration static headspace method for the determination of methane dissolved in seawater. Anal. Chem. 62, 2408-2412. doi: 10.1021/ac00220a030

Kikuchi, E., 1986. Contribution of the polychaete, Neanthes japonica (Izuka), to the oxygen uptake and carbon dioxide production of an intertidal mud-flat of the Nanakita River estuary, Japan. J. Exp. Mar. Biol. Ecol. 97, 81-93. doi: 10.1016/0022-0981(86)90069-9

Kristensen, E., Bouillon, S., Dittmar, T., Marchand C., 2008. Organic carbon dynamics in mangrove ecosystems: a review. Aquat. Bot. 2, 201-219. doi: 10.1016/j.aquabot.2007.12.005

Lafleur, P.M., Moore, T.R., Roulet, N.T., Frolking, S., 2005. Ecosystem respiration in a cool temperate bog depends on peat temperature but not water table. Ecosystems 8, 619-629. doi: 10.1007/s10021-003-0131-2

Liikanen, A.N.U., Murtoniemi, T., Tanskanen, H., Väisänen, T., Martikainen, P.J., 2002. Effects of temperature and oxygen availability on greenhouse gas and nutrient dynamics in sediment of a eutrophic mid-boreal lake. Biogeochemistry. 59(3), 269-286. doi: 10.1023/A:101601552

Molnar, N., Welsh, D.T., Marchand, C., Deborde, J., Meziane, T., 2013. Impacts of shrimp farm effluent on water quality, benthic metabolism and N-dynamics in a mangrove forest (New Caledonia). Estuar. Coast. Shelf S. 117, 12-21. doi: 10.1016/j.ecss.2012.07.012

Mosier, A.R., 1998. Soil processes and global change. Biol. Fertil. Soils. 27(3), 221-229. doi: 10.1007/s003740050

Morse, J.W., Rowe, G.T., 1999. Benthic biogeochemistry beneath the Mississippi River plume. Estuaries. 22(2), 206-214. doi: 10.2307/1352977

Mu, D., Yuan, D.K., Feng, H., Xing, F.W., Teo, F.Y., Li, S.Z., 2017. Nutrient fluxes across sediment-water interface in Bohai Bay Coastal Zone, China. Mar. Pollut. Bull. 114(2), 705-714. doi: 10.1016/j.marpolbul.2016.10.056

Müller, D., Warneke, T., Rixen, T., Müller, M., Mujahid, A., Bange, H.W., Notholt, J., 2016. Fate of terrestrial organic carbon and associated CO_2 and CO emissions from two Southeast Asian estuaries. Biogeosciences. 13, 691-705. doi:10.5194/bg-13-691-2016

Myhre, G., Shindell, D., Bréon, F.-M., Collins, W., Fuglestvedt, J., Huang, J., Koch, D., Lamarque, J.-F., Lee, D., Mendoza, B., Nakajima, T., Robock, A., Stephens, G., Takemura, T., Zhang, H., 2013. Anthropogenic and Natural Radiative Forcing, in: Stocker, T., Qin, D., Plattner, G.-K., Tignor, M., Allen, S., Boschung, J., Nauels, A., Xia, Y., Bex, V., Midgley, [Eds.]. Climate Change 2013: The Physical Science Basis. Contribution of Working Group I to the Fifth Assessment Report of the Intergovernmental Panel on Climate Change. Cambridge University Press, Cambridge, United Kingdom and New York, NY, USA.

Neal, C., House, W.A., Jarvie, H.P., Eatherall, A., 1998. The significance of dissolved carbon dioxide in major lowland rivers entering the North Sea. Sci. Total. Environ. 210-211, 187-203. doi: 10.1016/S0048-9697(98)00012-6

Ogrinc, N., Lojen, S., Faganeli, J., 2002. A mass balance of carbon stable isotopes in an organic-rich methane-producing lacustrine sediment (Lake Bled, Slovenia). Global. Planet. Change, 33, 57-72. doi: 10.1016/S0921-8181(02)00061-9

Raymond, P.A., Hartmann, J., Lauerwald, R., Sobek, S., McDonald, C., Hoover, M., Butman, D., Striegl, R., Mayorga, E., Humborg, C., Kortelainen, P., Durr, H., Meybeck, M., Ciais, P., Guth, P., 2013. Global carbon dioxide emissions from inland waters. Nature 503, 355-359. doi: 10.1038/nature12760

Schrier-Uijl, A.P., Veraart, A.J., Leffelaar, P.A., Berendse, F., Veenendaal, E.M., 2011. Release of CO_2 and CH_4 from lakes and drainage ditches in temperate wetlands. Biogeochemistry 102, 265-279. doi: 10.1007/s10533-010-9440-7

Sidik, F., Lovelock, C.E., 2013. CO_2 efflux from shrimp ponds in Indonesia. PLOS ONE. 8(6), e66329. doi:10.1371/journal.pone.0066329

Silva, K.R., Wasielesky, Jr.W., Abreu, P.C., 2013. Nitrogen and phosphorus dynamics in the biofloc production of the Pacific white shrimp, *Litopenaeus vannamei*. J. Word Aquacult. Soc. 44(1), 30-41. doi: 10.1111/jwas.12009

Sun, Z.G., Wang, L.L., Tian, H.Q., Jiang, H.H., Mou, X.J., Sun, W.L., 2013. Fluxes of nitrous oxide and methane in different coastal *Suaeda salsa* marshes of the Yellow River estuary, China. Chemosphere. 90(2), 856-865. doi: 10.1016/j.chemosphere.2012.10.004

Tan, Y.J., 2014. The greenhouse gases emission and production mechanism from river sediment in Shanghai. Thesis, East China Normal University, Shanghai. (in Chinese)

Tangen, B.A., Finocchiaro, R.G., Gleason, R.A., Dahl, C.F., 2016. Greenhouse gas fluxes of a shallow lake in south-central North Dakota, USA. Wetlands 36, 779-787. doi: 10.1007/s13157-016-0782-3

Tonetta, D., Staehr, P.A., Petrucio, M.M., 2017. Changes in CO_2 dynamics related to rainfall and water level variations in a subtropical lake. Hydrobiologia. 794(1), 109-123. doi: 10.1007/s1075

Tong, C., Morris, J.T., Huang, J.F., Xu, H., Wan, S.A., 2018. Changes in pore-water chemistry and methane emission following the invasion of *Spartina alterniflora* into an oliogohaline marsh. Limnol. Oceanogr. 63, 384-396. doi: 10.1002/lno.10637

Tong, C., Wang, W.Q., Zeng, C.S., Marrs, R., 2010. Methane emissions from a tidal marsh in the Min River estuary, southeast China. J. Environ. Sci. Heal. A. 45, 506-516. doi: 10.1080/10934520903542261

Tong, C., Wang, W.Q., Huang, J.F., Gauci, V., Zhang, L.H., Zeng, C.S., 2012. Invasive alien plants increase CH_4 emissions from a subtropical tidal estuarine wetland. Biogeochemistry. 111, 677-693. doi: 10.1007/s10533-012-9712-5

Urban, N.R., Dinkel, C., Wehrli, B., 1997. Solute transfer across the sediment surface of a eutrophic lake: I. Pore water profiles from dialysis samplers. Aquatic. Sci. 59(1), 1-25. doi: 10.1007/BF02522546

Vachon, D., Lapierre, J.F., Del Giorgio, P.A., 2016. Seasonality of photochemical dissolved organic carbon mineralization and its relative contribution to pelagic CO_2 production in northern lakes. J. Geophys. Res. Biogeosci. 121, 864-878. doi: 10.1002/2015JG003244

Vreča, P., 2003. Carbon cycling at the sediment-water interface in a eutrophic mountain lake (Jezero na Planini pri Jezeru, Slovenia). Org. Geochem. 34(5), 671-680. doi: 10.1016/S0146-6380(03)00022-6

Wallin, M., Buffam, I., Oquist, M., Laudon, H., Bishop., K., 2010. Temporal and spatial variability of dissolved inorganic carbon in a boreal stream network: Concentrations and downstream fluxes. J. Geophys. Res-Biogeo. 115, G02014. doi: 10.1029/2009jg001100

Wanninkhof, R., 1992. Relationship between wind speed and gas exchange over the ocean. J. Geophys. Rese-Oceans. 97(C5), 7373-7382. doi: 10.3878/j.issn.1006-9895.2012.11182

Weyhenmeyer, G.A., Kosten, S., Wallin, M.B., Tranvik, L.J., Jeppesen, E., Roland, F., 2015. Significant fraction of CO_2 emissions from boreal lakes derived from hydrologic inorganic carbon inputs. Nat. Geosci. 8(12), 933-936. doi: 10.1038/ngeo2582

Wiesenburg, D.A., Guinasso Jr., N.L., 1979. Equilibrium solubilities of methane, carbon dioxide, and hydrogen in water and sea water. J. Chem. Eng. Data. 24, 356-360. doi: 10.1021/je60083a006

Wollast, R., 1993. Interactions of carbon and nitrogen cycles in the coastal zone. In: Wollast, R., F. T. Mackenzie, and L. Chou [Eds.], Interactions of C, N, P and S Biogeochemical Cycles and Global Change, NATO ASI Series, Series 1: Global Environmental Change 4. Springer-Verlag, Berlin and Heidelberg, pp. 195-210.

World Meteorological Organization, 2018. WMO Greenhouse Gas Bulletin No. 14. https://library.wmo.int/doc_num.php?explnum_id=5455.

Wu, H., Peng, R., Yang, Y., He, L., Wang, W.Q., Zheng, T.L., Lin, G.H., 2014. Mariculture pond influence on mangrove areas in south China: Significantly larger nitrogen and phosphorus loadings from sediment wash-out than from tidal water exchange. Aquaculture. 426, 204-212. doi: 10.1016/j.aquaculture.2014.02.009

Xiang, J., Liu, D.Y., Ding, W.X., Yuan, J.J., Lin, Y.X., 2015. Invasion chronosequence of *Spartina alterniflora* on methane emission and organic carbon sequestration in a coastal salt marsh. Atmos. Environ. 112, 72-80. doi: 10.1016/j.atmosenv.2015.04.035

Xing, Y.P., Xie, P., Yang, H., Ni, L.Y., Wang, Y.S., Tang, W.H., 2004. Diel variation of methane fluxes in summer in a eutrophic subtropical lake in china. Journal of Freshwater Ecology 19, 639-644.

Xing, Y., Xie, P., Yang, H., Ni, L., Wang, Y., Rong, K., 2005. Methane and carbon dioxide fluxes from a shallow hypereutrophic subtropical lake in china. Atmospheric Environment 39, 5532-5540.

Xing, Y.P., Xie, P., Yang, H., Wu, A.P., Ni, L.Y., 2006. The change of gaseous carbon fluxes following the switch of dominant producers from macrophytes to algae in a shallow subtropical lake of china. Atmospheric Environment 40, 8034-8043.

Xiong, Y.H., Wang, F., Guo, X.T., Liu, F., Dong, S.L., 2017. Carbon dioxide and methane fluxes across the sediment-water interface in different grass carp *Ctenopharyngodon idella* polyculture models. Aquacult. Environ. Interact. 9, 45-56. doi: 10.3354/aei00214.

Yang, H., 2014. China must continue the momentum of green law. Nature 509, 535-353.

Yang, H., Andersen, T., Dörsch, P., Tominaga, K., Thrane, J.-E., Hessen, D.O., 2015a. Greenhouse gas metabolism in Nordic boreal lakes. Biogeochemistry 126, 211-225.

Yang H., Flower R.J. 2012. Potentially massive greenhouse-gas sources in proposed tropical dams. Frontiers in Ecology and the Environment 10, 234-235.

Yang, H., Xie, P., Ni, L., Flower, R.J., 2011. Underestimation of CH_4 emission from freshwater lakes in china. Environmental Science Technology 45, 4203-4204.

Yang, H., Xing, Y., Xie, P., Ni, L., Rong, K. 2008. Carbon source/sink function of a subtropical, eutrophic lake determined from an overall mass balance and a gas exchange and carbon burial balance. Environmental Pollution 151, 559-568.

Yang, P., He, Q.H., Huang, J.F., Tong, C., 2015b. Fluxes of greenhouse gases at two different aquaculture ponds in the coastal zone of southeastern China. Atmos. Environ. 115, 269-277. doi: 10.1016/j.atmosenv.2015.05.067

Yang, P., Lai, D.Y.F., Jin, B.S., Bastviken, D., Tan, L.S., Tong, C., 2017a. Dynamics of dissolved nutrients in the aquaculture shrimp ponds of the Min River estuary, China: Concentrations, fluxes and environmental loads. Sci. Total Environ. 603-604, 256-267. doi: 10.1016/j.scitotenv.2017.06.074

Yang, P., Bastviken, D., Jin, B.S., Mou, X.J., Tong, C., 2017b. Effects of coastal marsh conversion to shrimp aquaculture ponds on CH_4 and N_2O emissions. Estuar. Coast. Shelf S. 199, 125-131. doi: 10.1016/j.ecss.2017.09.023

Yang, P., Lai, D.Y.F., Huang, J.F., Tong, C., 2017c. Effect of drainage on CO_2, CH_4, and N_2O fluxes from aquaculture ponds during winter in a subtropical estuary of China. J. Environ. Sci. 65, 72-82. doi: 10.1016/j.jes.2017.03.024

Yang, P., Jin, B.S., Tan, L.S., Tong, C., 2018a. Spatial-temporal variations of water column dissolved carbon concentrations and dissolved carbon flux at the sediment-water interface in the shrimp ponds from two subtropical estuaries. Acta Ecol. Sinica. 38(6). doi: 10.5846/stxb201702210284. (in Chinese).

Yang, P., Zhang, Y.F., Lai, D.Y.F., Tan, L.S., Jin, B.S., Tong, C., 2018b. Fluxes of carbon dioxide and methane across the water-atmosphere interface of aquaculture shrimp ponds in two subtropical estuaries: The effect of temperature, substrate, salinity and nitrate, *Sci. Total Environ.*, 635, 1025-1035.

Yao, Y.C., Ren, C.Y., Wang, Z.M., Wang, C., Deng, P.Y., 2016. Monitoring of salt ponds and aquaculture ponds in the coastal zone of China in 1985 and 2010. Wet. Sci. 14(6), 874-882 (in Chinese).

Zhang, G.L., Zhang, J., Liu, S.M., Ren, J.L., Zhao, Y.C., 2010a. Nitrous oxide in the Changjiang (Yangtze River) Estuary and its adjacent marine area: riverine input, sediment release and atmospheric fluxes. Biogeosciences. 7, 3505-3516. doi: 10.5194/bg-7-3505-2010

Zhang, L., Wang, L., Yin, K.D., Lü, Y., Zhang, D.R., Yang, Y.Q., Huang, X.P., 2013. Pore water nutrient characteristics and the fluxes across the sediment in the Pearl River estuary and adjacent waters, China. Estuar. Coast. Shelf S. 133, 182-192. doi: 10.1016/j.ecss.2013.08.028

Zhang, Y.H., Ding, W.X., Cai, Z.C., Valerie, P., Han, F.X., 2010b. Response of methane emission to invasion of *Spartina alterniflora* and exogenous N deposition in the coastal salt marsh. Atmos. Environ. 44, 4588-4594. doi: 10.1016/j.atmosenv.2010.08.012

Zheng, Z.M., Dong, S.L., Tian, X.L., Wang, F., Gao, Q.F., Bai, P.F., 2009. Sediment water fluxes of nutrients and dissolved organic carbon in extensive sea cucumber culture ponds. Clean−Soil Air Water. 37, 218-224. doi: 10.1002/clen.200800193

Zhong, D.S., Wang, F., Dong, S.L., Li, L., 2015. Impact of *Litopenaeus vannamei* bioturbation on nitrogen dynamics and benthic fluxes at the sediment-water interface in pond aquaculture. Aquacult. Int. 23(4), 967-980. doi: 10.1007/s1049

Fig. 1. Location of the study area and sampling sites in the Min River Estuary and Jiulong River Estuary, Fujian, Southeast China (Yang et al., 2018b).

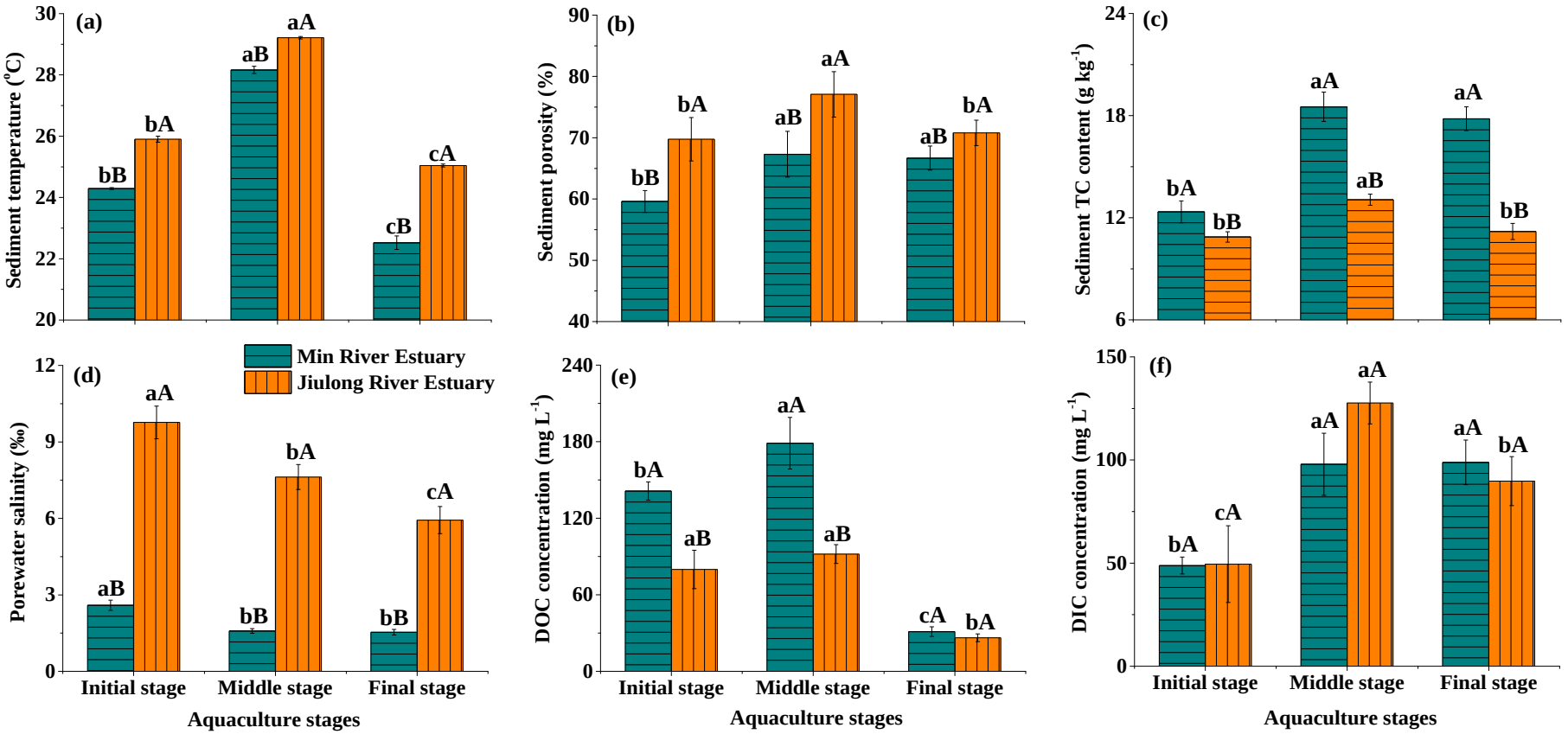

Fig. 2. Variations in (**a**) temperature, (**b**) porosity, and (**c**) total carbon (TC) in surface (0–15 cm) sediments, and (**d**) salinity, (**e**) dissolved organic carbon (DOC), and (**f**) dissolved inorganic carbon (DIC) concentrations in the sediment porewater of shrimp ponds at the Min River Estuary (MRE) and Jiulong River Estuary (JRE). Bars represent means ± 1 SE (n = 9). Different lowercase and uppercase letters on the bars indicate significant differences among different growth stages and estuaries, respectively ($p < 0.05$).

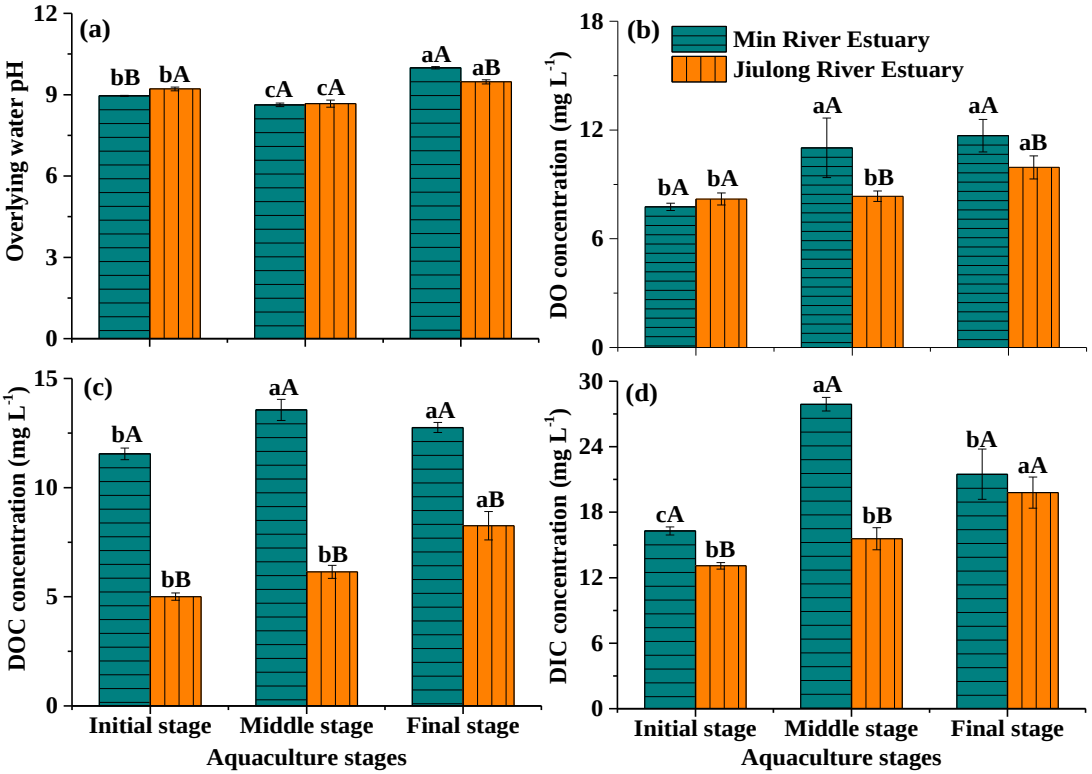

873

874 **Fig. 3.** Variations in (**a**) pH, (**b**) dissolved oxygen (DO), (**c**) dissolved organic carbon (DOC) and
875 (**d**) dissolved inorganic carbon (DIC) in the overlying water of shrimp ponds at the Min River
876 Estuary and Jiulong River Estuary. Bars represent means ± 1 SE (n = 9). Different lowercase and
877 uppercase letters on the bars indicate significant differences among different growth stages and
878 estuaries, respectively ($p < 0.05$).

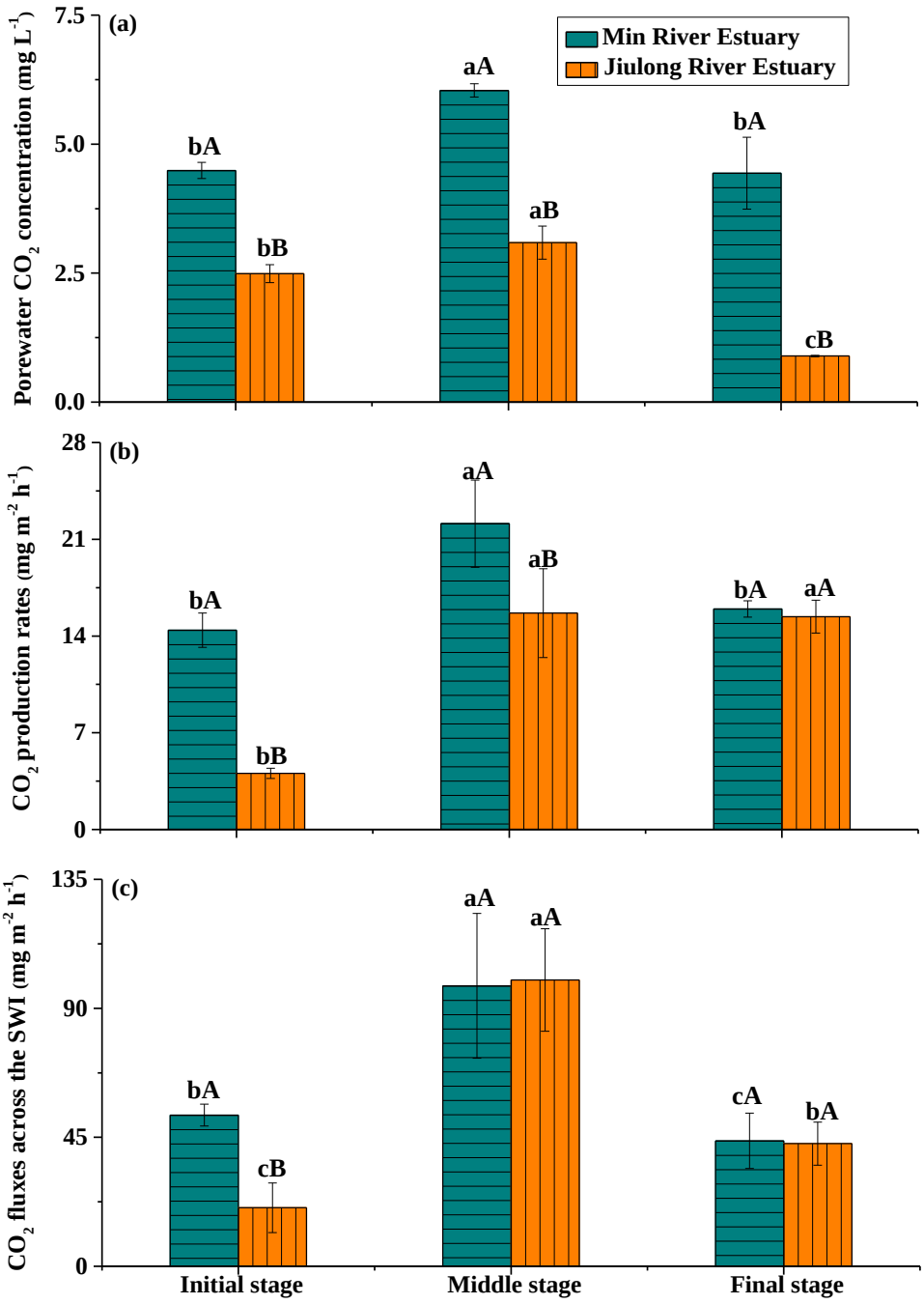

879

880 **Fig. 4.** Variations in (**a**) sediment porewater CO_2 concentration, (**b**) overlying water CO_2
881 production rate (CO_{2_WP}), and (**c**) CO_2 fluxes across the sediment-water interface (SWI) of shrimp
882 ponds at the Min River Estuary and Jiulong River Estuary. Bars represent means ± 1 SE (n = 9).
883 Different lowercase and uppercase letters on the bars indicate significant differences among
884 different growth stages and estuaries, respectively ($p < 0.05$).

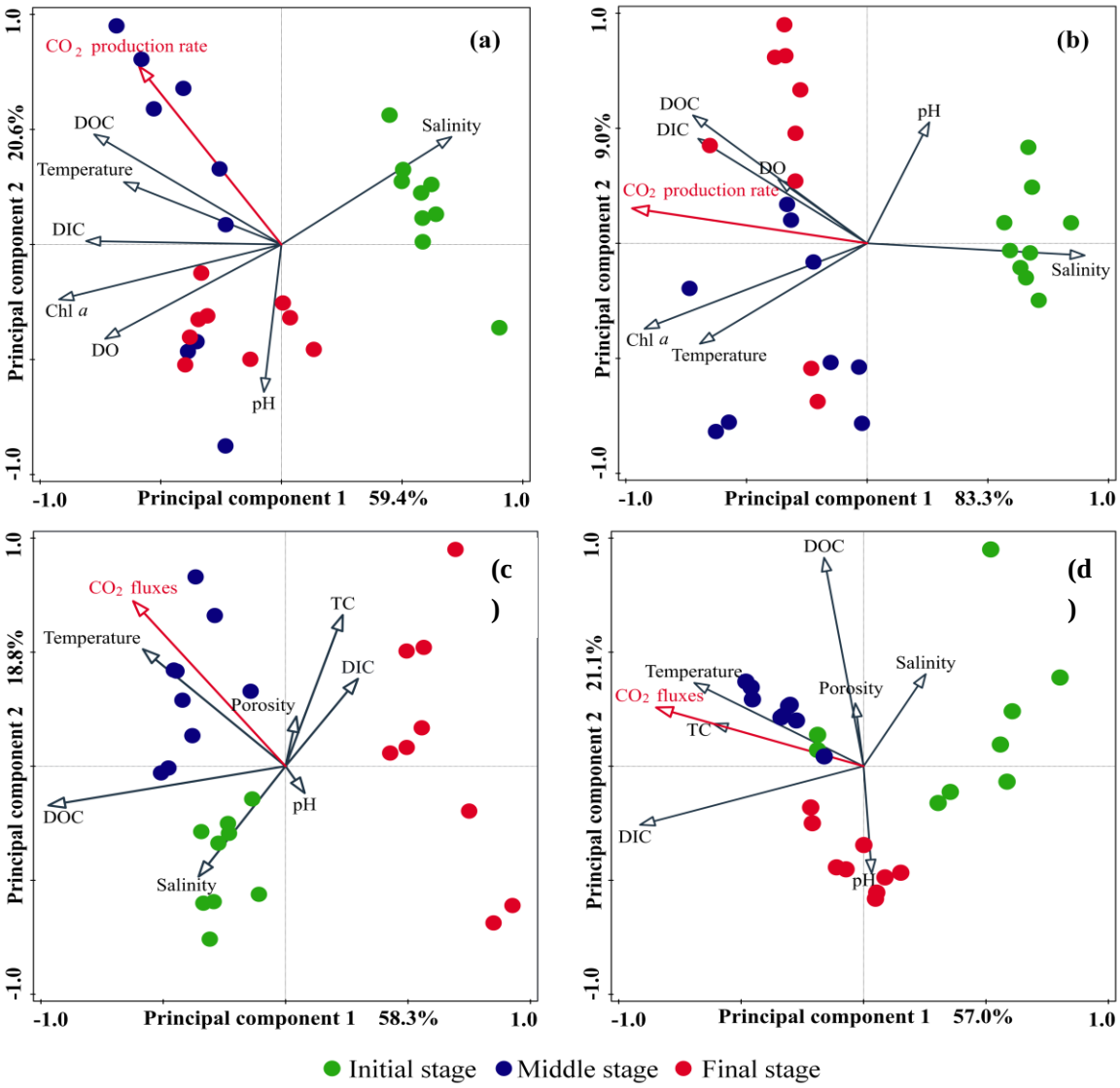

885

886 **Fig. 5.** The principal component analysis biplots of the CO_2 production rates in the overlying
887 water, CO_2 fluxes across the SWI and various environmental factors of (**a, c**) Min River Estuary
888 and (**b, d**) Jiulong River Estuary ponds, showing the loadings of environmental factors (arrows)
889 and the scores of observations in different aquaculture stages (points).

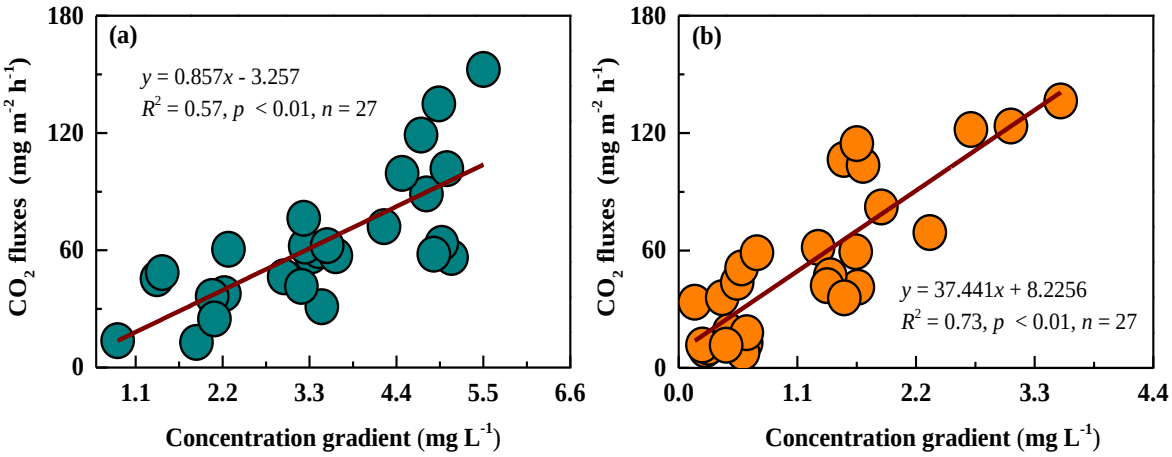

890

891 **Fig. 6.** Relationships between CO_2 fluxes and CO_2 concentration gradients across the SWI of
892 shrimp ponds at the (**a**) Min River Estuary and (**b**) Jiulong River Estuary. The solid lines represent
893 the best-fit linear regression ($p < 0.01$).

894

Table 1

Results of two-way ANOVA of the effects of estuaries and aquaculture stages on sediment porewater CO_2 concentrations, CO_2 production rates, and CO_2 fluxes across the SWI of shrimp ponds at the Min River Estuary and Jiulong River Estuary.

	df	Porewater CO_2	CO_2 production	CO_2 fluxes
Estuaries	1	67.240**	18.674**	1.980
Aquaculture stages	2	10.162*	17.889**	33.557**
Aquaculture stages × Estuaries	2	1.700	4.513*	3.094

** $p < 0.001$, * $p < 0.01$.

Table 2

Pearson correlation coefficients for porewater CO_2 concentrations and various physico-chemical parameters of porewater and sediments in the shrimp ponds of the Min River Estuary (MRE) and Jiulong River Estuary (JRE).

Estuary	Porewater			Sediment			
	DOC	DIC	Salinity	Temperature	Porosity	TC	pH value
MRE	0.451*	NS	NS	0.398*	NS	NS	-0.392*
JRE	0.486**	NS	NS	0.672**	NS	0.411*	-0.528**

NS denotes "nonsignificant relationship". [a] n = 27 for environmental variables and porewater CO_2 concentrations at shrimp ponds in each estuary. The symbols * and ** denote significant correlations at $p < 0.05$ and 0.01, respectively.

907 **Table 3**

908 Results of stepwise multiple linear regression analysis between CO_2 production rates and various
909 environmental parameters in the overlying water of the Min River Estuary (MRE) and Jiulong
910 River Estuary (JRE).

Estuary	Regression equations	*F*-value	R^2	*p*-value
MRE	$Y = 3.949X_{DOC} - 2.636X_{pH} - 8.105$	38.161	0.761	< 0.001
JRE	$Y = -1044X_{salinity} + 0.672X_{DIC} + 10.373$	26.360	0.687	< 0.001

Table 4

Results of stepwise multiple linear regression analysis between CO_2 fluxes across the SWI and various environmental parameters in the pond sediments of the Min River Estuary (MRE) and Jiulong River Estuary (JRE).

Estuary	Regression equations	*F*-value	R^2	*p*-value
MRE	$Y = 8.184X_{Temperature} - 0.502X_{DIC} + 3.555X_{TC} - 152.525$	15.006	0.662	< 0.001
JRE	$Y = 22.129X_{Temperature} - 546.524$	56.542	0.693	< 0.001

Table 5

A summary of CO_2 fluxes (mg m^{-2} h^{-1}) across the sediment-water interface in different aquatic ecosystems (e.g. lakes, reservoirs, rivers, drainage ditch, aquaculture ponds, and others).

Ecosystems Type	Study Site	Average Depth (m)	Range	Reference
Lake	Bled Lake, Slovenia	17.9	9.2	Ogrinc et al., 2002
	Stechlin Lake, Germany	22.8	4.4 – 6.2	Casper et al., 2003
	Kevatön Lake, Finland	2.3	20.2 – 56.8	Liikanen et al., 2002
	Baldeg Lake, Switzerland	56 – 65	3.9 – 13.2	Urban et al., 1997
Reservoir	Wilcza Wola Reservoir, Poland	2.6	2.2 – 3.9	Gruca-Rokosz et al., 2011
	Solina Reservoir, Poland	22.0	2.2 –2.6	Gruca-Rokosz et al., 2011
	Rzeszów Reservoir, Poland	0.5 – 6.0	0.9 – 83.2	Gruca-Rokosz and Tomaszek, 2015
	Lobo Broa Reservoir, Brazil	3.0	16.3 – 47.9	Adams, 2005
River/Estuary	Palmones River estuary	---	16.7 – 313.7	Claverol et al., 1997
	Mississippi River estuary	---	31.2 – 102.5	Morse and Rowe, 1999
	Kertinge Nor River estuary	---	128.5 – 155.8	Hansen and Kristensen, 1997
	Shanghai river network, China	1.35 – 4.0	-43.6 – 52.8	Tan et al., 2014
Intertidal mudflat	Nanakita River, Japan	---	117.0 – 533.7	Kikuchi, 1986
Drainage ditch	Netherlands	0.25 – 0.90	69.5 –198.9	Schrier-Uijl et al., 2011
Aquaculture pond	Shandong Province, China	1.8	19.8 – 124.1	Xiong et al., 2017
	Min River estuary, China	1.3	43.6 – 97.7	Present study
	Jiulong River estuary, China	1.5	20.2 – 99.9	Present study

"---" indicated No data

919

920